Outflanking Bandwidth Limitations for Terahertz Generation in Silicon Metasurfaces

Andrea Tognazzi, Davide Rocco, *Member, IEEE*, Paolo Franceschini, Alfonso Carmelo Cino, and Costantino De Angelis

***Abstract*—Terahertz (THz) radiation is of utmost interest for applications ranging from communications to safety and biological spectroscopy. However, the generation of THz frequencies above 5 THz is challenging due to absorption in crystals and pump bandwidth requirements. Here, a silicon-based metasurface, featuring resonant modes in the near-infrared (NIR), is employed as nonlinear platform for the generation of THz radiation via degenerate four wave mixing process. We show that it is feasible to achieve on demand frequency generation by sweeping the central wavelength of a visible narrowband pulse and keeping the NIR pump beam unaltered, thus avoiding the need of broadband pump pulses. The usage of a metasurface allows to drastically reduce the absorption in the THz region. Our results pave the way to broadband spectroscopy in the THz region.**

***Index Terms*—Terahertz, four wave mixing, nonlinear optics, metasurfaces.**

I. Introduction

TERAHERTZ (THz) frequencies correspond to the spectral range where the optical response ascribed to molecular motion appears. This allows spectroscopic fingerprinting of biological molecules, drugs, and materials for applications spanning security screening, quality control, and agricultural diagnostics [1], [2], [3]. As in all spectroscopic applications, probing a large spectral range is desirable. Such broad frequency range can be achieved either by employing a broadband source or by sweeping the spectral position of an extremely narrowband source over the desired frequency range. However, THz sources are not readily available and are either hardly tunable single frequency lasers, such as quantum cascade lasers [4], or require ultrashort laser pulses to operate photo-conductive antennas (PCAs) or perform difference frequency generation (DFG) in crystals. Although PCAs offer a relatively compact and easy to operate THz pulse source [5], the maximum bandwidth is still limited to few THz (tipically < 3 THz). Intrapulse frequency generation in nonlinear crystals, such as ZnTe or GaP, are a well established alternative to achieve higher THz frequencies [6]. However, several gaps in the generated spectra are present and the maximum achievable THz frequencies are limited by the absorption in crystals and the pump pulse bandwidth. The absorption effects can be reduced by thinning the crystal, thus reducing the propagation length. This approach has been successfully employed to achieve THz generation up to 7 THz in a 400-μm-thick GaP slab [7] or 500-nm-thick $LiNbO_3$ film [8]. However, thinner crystals make no use of phase-matching and are inherently less efficient. The additional limiting factor is the pump pulse bandwidth, which must be broad enough to allow intrapulse DFG. Assuming a typical gaussian-like pulse shape, the spectral power available for high THz frequency generation rapidly decreases. To overcome the limitations of available bandwidth, dual beam DFG [9], [10], [11] and four-wave

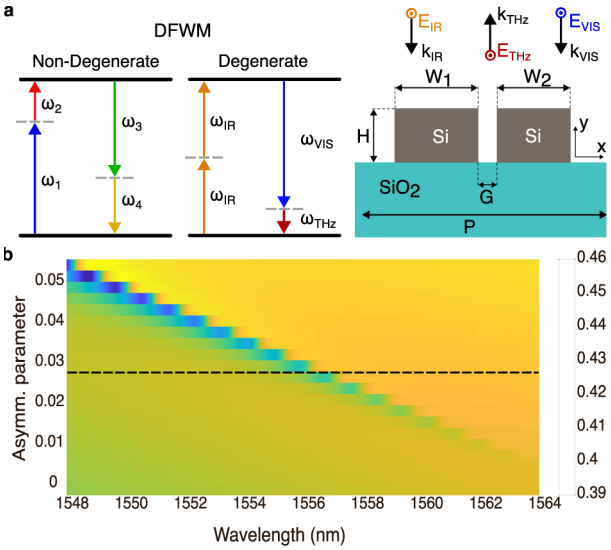

Fig. 1. a. Schematic of the difference four wave mixing processes and the unit cell of the investigated metasurface. b. Reflectivity as a function of the asymmetry parameter (α) and the wavelength. The dashed line corresponds to the value of α employed for nonlinear simulations.

Received 23 January 2026; revised 13 March 2026; accepted 29 April 2026. Date of publication 4 May 2026; date of current version 13 May 2026. The work of Davide Rocco was supported by the European Union (EU)–Next Generation EU, Mission 4 Component 1–PRIN 2022 Project GRACE6G CUP D53D23001250001 under Grant 2022H7RR4F. The work of Alfonso Carmelo Cino was supported by the University of Palermo through "Fondo Finalizzato alla Ricerca 2025." *(Corresponding author: Andrea Tognazzi.)*

Andrea Tognazzi is with the Dipartimento di Ingegneria, Universitá degli Studi di Palermo, 90128 Palermo, Italy, and also with the Istituto Nazionale di Ottica—Consiglio Nazionale delle Ricerche (INO-CNR), 25123 Brescia, Italy (e-mail: andrea.tognazzi@unipa.it).

Davide Rocco, Paolo Franceschini, and Costantino De Angelis are with the Istituto Nazionale di Ottica—Consiglio Nazionale delle Ricerche (INO-CNR), 25123 Brescia, Italy, and also with the Dipartimento di Ingegneria dell'Informazione, Universitá degli Studi di Brescia, 25123 Brescia, Italy.

Alfonso Carmelo Cino is with the Dipartimento di Ingegneria, Universitá degli Studi di Palermo, 90128 Palermo, Italy.

Color versions of one or more figures in this letter are available at https://doi.org/10.1109/LPT.2026.3690029.

Digital Object Identifier 10.1109/LPT.2026.3690029

mixing [12], [13], [14], [15], [16], [17] configuration, even involving plasmas as nonlinear medium, have been proposed. However, the limitations due to absorption in the THz region still remain. In the past, solutions based on nanophotonics devices have been proposed to overcome the difficulties related to phase matching over long distances by engineering the dispersion of waveguides or optical fibers [18], [19], [20], [21]. However, such approaches do not allow to achieve broadband phase matching and are not easily tunable. On the other hand, metasurfaces have been demonstrated as viable platforms to generate frequencies above 6 THz by intrapulse DFG [8], [22], where the enhancement is usually provided by the resonant behavior of the nonlinear polarizability close to phonon modes. The generation of such broadband THz pulses requires ultrashort laser pulses with large frequency content that poorly exploits high quality factor (Q-factor) modes, such as quasi-bound states in the continuum (qBIC), which provide strong field enhancement [23]. In this work, we propose a tunable THz radiation source based on a degenerate difference four wave mixing (DFWM) process in a silicon (Si) metasurface consisting in a one dimensional periodic grating featuring a high Q-factor qBIC mode in the NIR (Fig. 1a). The DFWM process is specifically designed to exploit as inputs two narrowband NIR pulses at frequency ω_{IR} (spectrally resonant to the BIC mode) and a visible pulse at $\omega_{VIS} \simeq 2\omega_{IR}$, such that the output radiation is generated at $\omega_{THz} = 2\omega_{IR} - \omega_{VIS}$. In this condition, when ω_{VIS} is spectrally varied by keeping ω_{IR} fixed (thus, ensuring strong nonlinear response), the frequency of the output THz radiation can be tuned. The identification of the geometrical condition ensuring the occurrence of the BIC modes in the desired spectral range and the demonstration of the tunability of the output THz radiation have been achieved via numerical simulation based on finite element method. Our results provide an alternative approach for broadband spectroscopy in the THz spectral range based on a tunable narrowband source.

II. Results

The investigated metasurface consists in a one-dimensional periodic grating structure (with period P) deposited on top of a SiO_2 substrate. As shown in Fig. 1a, the unit cell comprises two bars with different width (W_1 and W_2), same height H, and separated by a distance G. The width difference induces the symmetry-breaking that generates a qBIC resonance and its magnitude allows to control the qBIC spectral position and bandwidth. The grating is designed to support a qBIC resonance in the IR region. Fig. 1b shows the reflectivity as a function of the wavelength and the asymmetry parameter $\alpha = (W_1 - W_2)/W_1$ for $G = 40$ nm, $H = 200$ nm, $P = 650$ nm. In the following, we set $W_1 = 180$ nm and $W_2 = 175$ nm. The presence of a qBIC allows to improve frequency conversion by enhancing the local electric field inside the grating bars. We consider a DFWM process (Fig. 1a), where two narrowband NIR pulses at $\omega_{IR} \simeq \omega_{BIC}$ are combined with a VIS pulse at $\omega_{VIS} \simeq 2\omega_{IR}$ to generate an output radiation in the low-frequency spectral range at $\omega_{THz} = 2\omega_{IR} - \omega_{VIS}$. In the visible region we operate out of resonance (see Fig. 2b) and in the THz region the metasurface is not resonant (see Fig. 2c).

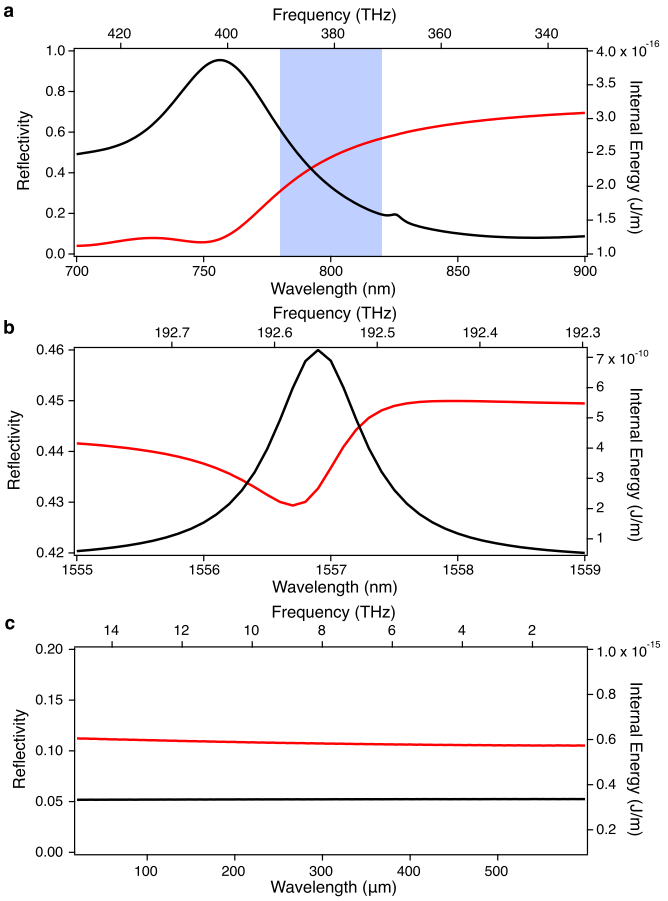

Fig. 2. Reflectivity (red lines, left axis) and Internal energy, $U = \int \epsilon |E|^2 dA$, (black lines, right axis) as a function of the wavelength in the visible (panel a), near infrared (panel b) and terahertz (panel c) regions at normal incidence. The light blue shaded area in panel a corresponds to the frequencies involved in the degenerate DFWM resulting in the frequency range in panel c.

Although triply resonant structures have been predicted to yield high conversion efficiencies [24], [25], [26], the generated spectra are extremely narrowband and not tunable. In our case, the nonlinear frequency conversion is boosted by the narrow resonance in the IR and the tunability is provided by the non resonant behavior in the other spectral regions. Even if the presence of broad resonances might be helpful to further increase the conversion efficiency, the research of such design is beyond the scope of this letter.

A. Numerical Model

The nonlinear response for a degenerate DFWM process with local third order susceptibility response should be calculated as:

$$\tilde{P}_i^{(3)}(\omega_{THz}) = \varepsilon_0 \chi_{ijkl}^{(3)} \left[(\tilde{E}_{j,IR} \circledast \tilde{E}_{k,IR}) \circledast \tilde{E}_{l,VIS}^{*} \right](\omega_{THz}), \quad (1)$$

where $\tilde{P}^{(3)}(\omega_{THz})$ is the i-th component of the third order nonlinear polarization at THz frequency ω_{THz}, $\chi_{jkl}^{(3)}$ are the third order susceptibility components, $\circledast$ stands for the convolution operation in frequency domain, and $\tilde{E}_{IR,VIS}$ are the electric fields components at $\omega_{IR,VIS}$. As previously observed, the energy of a laser pulse that couples to a qBIC is only that of the spectral components matching the qBIC bandwidth [27].

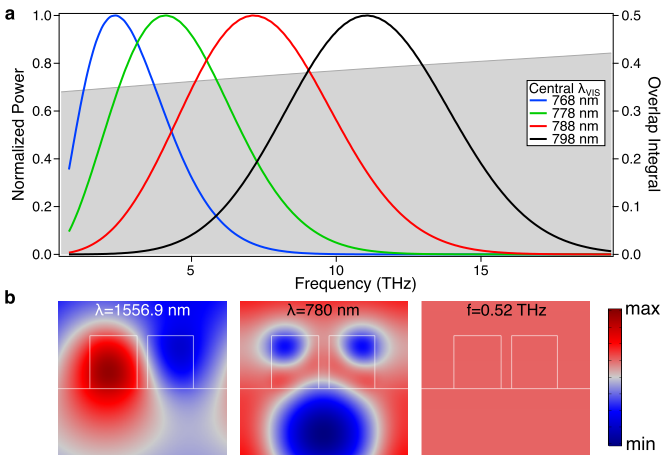

Fig. 3. a. Frequency-resolved power spectra (normalized units) of the output THz radiation for different values of λ_{VIS}. The shaded area corresponds to the overlap integral. b. Selected field profiles employed for the overlap integral calculation.

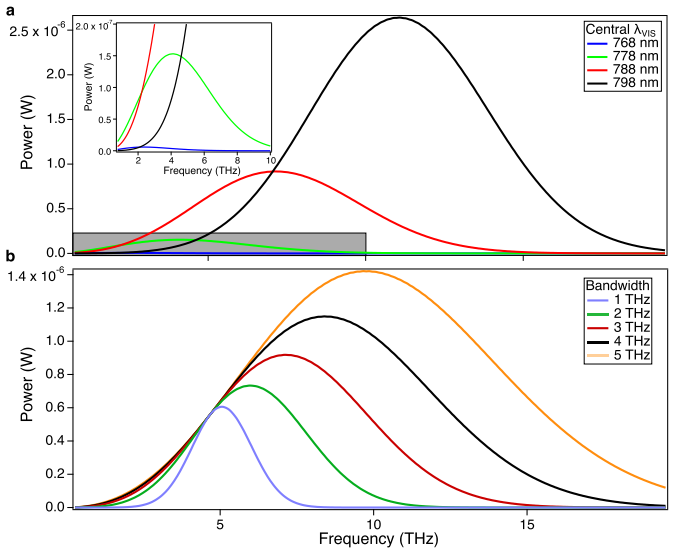

Fig. 4. Frequency-resolved power spectra of the output THz radiation for different values of λ_{VIS} and fixed bandwidth $\Delta\omega_{VIS}$ = 3 THz (panel a), and fixed λ_{VIS}=788 nm and different values of $\Delta\omega_{VIS}$ (panel b). The inset in a shows a zoom of the shaded gray area.

Indeed, degenerate four wave mixing involving two resonant photons at the qBIC leads to larger frequency conversion rather than non-resonant photons [28]. This drastically simplifies our model as qBIC can have extremely narrow bandwidth (< 0.1 THz, $Q \sim 2 \times 10^3$). Due to the coupling to the qBIC mode, the spectral components of the NIR pulse entering the nonlinear interaction can be approximated by a delta function, $\tilde{E}_{IR} \approx \delta(\omega - \omega_{BIC})$ [28]. Therefore, for a gaussian VIS pulse $\tilde{E}_{VIS} \propto \exp[-(\omega - \omega_{VIS})^2/\Delta\omega_{VIS}^2]$, Eq. 1 provides:

$$\tilde{P}^{(3)}(\omega) \propto \exp\left[-(\omega + 2\omega_{BIC} - \omega_{VIS})^2/\Delta\omega_{VIS}^2\right], \qquad (2)$$

where $\tilde{P}^{(3)}(\omega) \neq 0$ when ω is in the THz region.

We employ Comsol Multiphysics to perform frequency domain simulations and reconstruct the generated THz spectra under the undepleted pump approximation. The nonlinear results are obtained under the approximation that the only contribution to nonlinear interaction due to the IR frequencies is due to the qBIC mode. Under such approximation, we can obtain the THz spectra performing a parametric sweep over the visible frequencies only. Since silicon structures on the orders of few mm with similar geometry were reported in the literature [28], the simulations are performed in the frequency domain by imposing periodic boundary conditions at all frequency steps. The impinging electric field is always aligned along the bar direction (z-axis). The only non-zero term giving a contribution is $\chi^{(3)}_{zzzz} = 1 \times 10^{-17}$ m^2/V^2 [29]. Even though second order nonlinearity dispersion has been shown to lead to large efficiency enhancement in THz generation [22], we assume the third order susceptibility to be dispersionless and real-valued. The symmetry of the problem allows to perform 2D simulations of the transverse plane only. For computational reasons, the input intensity at ω_{BIC} is set to 10 kW/m^2 and that of the VIS pulse is weighted by a gaussian profile with peak value of 100 kW/m^2.

We consider a lossless case in the THz region (additional results including the effect of losses can be found in the Supplementary Material Document). The normalized output power of the generated THz radiation as a function of the generated frequency is shown in Fig. 3a. When $\omega_{VIS} \simeq 2\omega_{BIC}$, the maximum of the generated frequency is below 1 THz. Decreasing ω_{VIS} increases the peak THz frequency which is generated, showing the possibility to select the desired THz frequencies by properly tuning the pump visible pulse. As there are no resonances in the visible and THz regions, the overlap integral (shaded gray area in Fig. 3a) is almost constant over the entire region of interest. Fig. 3b shows the electric field distribution at 1556.9 nm (192.56 THz), 780 nm (384.35 THz) and 576523 nm (0.52 THz). Over one unit cell, the THz field is almost constant and the overlap integral is determined by the fields in the optical region. As can be seen by Fig. 4, the output power in the THz region rapidly increases when the visible pulse wavelength (λ_{VIS}) increases. This is due to the second time derivative of the nonlinear polarization term in the source term of the Maxwell's equation which results in a quartic dependence of the output power upon the frequency difference. Such effect is also evident in Fig. 4b where the central pulse frequency is kept constant and the bandwidth changes. We note that in such a case, the generated spectra can be described by the function $f(\omega) = \omega^4 \exp[-(\omega - \omega_0)^2/(\Delta\omega^2)]$, where ω is the frequency, ω_0 the central frequency of the gaussian and $\Delta\omega$ the bandwidth.

We emphasize that the involved frequencies in the DFWM process do not belong to the same pulse and thus large peak power values can be easily employed for the visible pump pulse. Moreover, the involved frequencies are commonly available outputs of commercial optical parametric amplifiers.

We propose an alternative approach to lift the requirements of broad pump pulses thus achieving a tunable THz source for spectroscopic applications. In contrast to spectroscopy methods based on parallel approach [30], where the frequency components are measured simultaneously (thus needing a broadband source), our idea promotes the serial approach, in which the individual frequency components are measured one

at a time by sweeping a narrowband source over a range of frequencies (see Fig. 1a). The proposed approach allows to achieve a relatively narrowband THz source which can be tuned over the desired frequency range by simply changing the central frequency of the pump pulses. This approach is especially significant for spectroscopic applications where the reflectivity/transmittivity spectra can be reconstructed by the separate narrowband spectra. Even though our approach relies on non-propagating modes and does not allow for phase matching, this limitation is not particularly restrictive, as phase matching cannot be effectively exploited in thin crystals either. However, in our case we can exploit the strong field localization to increase nonlinear frequency conversion. Compared to second order processes, where the spectral frequencies are contained in the same pulse, our approach allows to achieve higher spectral intensities at larger frequency differences. Moreover, the pump beam in the IR can be operated independently from the visible source. Additionally, since our approach is based on third order susceptibility, the restrictions on material selection are lifted.

III. Conclusion

We propose and theoretically investigate THz generation exploiting degenerate DFWM in a silicon metasurface. We show that operating close to a qBIC allows to drastically simplify the description of the problem and achieve a complete tunability over the THz region by properly tuning only the VIS pump pulse. The main advantage is that the proposed approach involves peak frequencies, rather than frequencies in the same pulse, which makes possible to exploit higher spectral power for large frequency differences above 6 THz. The use of metasurfaces improves the ease of tunability and reduces the absorption at the generated THz frequencies due to propagation in the material. Moreover, the use of third order susceptibility for THz generation paves the way to new materials beyond the non-centrosymmetric ones.

References

[1] X. Chen et al., "Terahertz (THz) biophotonics technology: Instrumentation, techniques, and biomedical applications," *Chem. Phys. Rev.*, vol. 3, no. 1, Mar. 2022, Art. no. 011311, doi: 10.1063/5.0068979.

[2] J. Yu, X. Liu, G. Manago, T. Tanabe, S. Osanai, and K. Okubo, "New terahertz wave sorting technology to improve plastic containers and packaging waste recycling in Japan," *Recycling*, vol. 7, no. 5, p. 66, Sep. 2022.

[3] L. T. Wedage, B. Butler, S. Balasubramaniam, Y. Koucheryavy, J. M. Jornet, and M. C. Vuran, "Climate change sensing through terahertz communication infrastructure: A disruptive application of 6G networks," *IEEE Netw.*, vol. 38, no. 3, pp. 261–268, May 2024.

[4] L. Gao, C. Feng, and X. Zhao, "Recent developments in terahertz quantum cascade lasers for practical applications," *Nanotechnol. Rev.*, vol. 12, no. 1, Sep. 2023, Art. no. 20230115.

[5] N. M. Burford and M. O. El-Shenawee, "Review of terahertz photoconductive antenna technology," *Opt. Eng.*, vol. 56, no. 1, Jan. 2017, Art. no. 010901.

[6] J. Hebling, A. G. Stepanov, G. Almási, B. Bartal, and J. Kuhl, "Tunable THz pulse generation by optical rectification of ultrashort laser pulses with tilted pulse fronts," *Appl. Phys. B, Lasers Opt.*, vol. 78, no. 5, pp. 593–599, Mar. 2004.

[7] I. D. Vugmeyster, J. F. Whitaker, and R. Merlin, "GaP based terahertz time-domain spectrometer optimized for the 5-8 THz range," *Appl. Phys. Lett.*, vol. 101, no. 18, Oct. 2012, Art. no. 181101.

[8] L. Carletti et al., "Nonlinear THz generation through optical rectification enhanced by phonon–polaritons in lithium niobate thin films," *ACS Photon.*, vol. 10, no. 9, pp. 3419–3425, Aug. 2023.

[9] Y. J. Ding, "Progress in terahertz sources based on difference-frequency generation [invited]," *J. Opt. Soc. Amer. B, Opt. Phys.*, vol. 31, no. 11, p. 2696, Oct. 2014.

[10] P. Liu et al., "Widely tunable and monochromatic terahertz difference frequency generation with organic crystal 2-(3-(4-hydroxystyryl)-5,5-dime-thylcyclohex-2-enylidene) malononitrile," *Appl. Phys. Lett.*, vol. 108, no. 1, Jan. 2016, Art. no. 011104.

[11] W. Li et al., "Dual-wavelength generator for high-efficiency difference frequency generation of a terahertz wave," *Opt. Lett.*, vol. 50, no. 6, p. 1791, Mar. 2025.

[12] A. Houard, Y. Liu, B. Prade, and A. Mysyrowicz, "Polarization analysis of terahertz radiation generated by four-wave mixing in air," *Opt. Lett.*, vol. 33, no. 11, p. 1195, May 2008.

[13] M. Koys, E. Noskovicova, D. Velic, and D. Lorenc, "Nonphasematched broadband THz amplification and reshaping in a dispersive chi(3) medium," *Opt. Exp.*, vol. 25, no. 12, p. 13872, Jun. 2017.

[14] J. Buldt, H. Stark, M. Müller, C. Grebing, C. Jauregui, and J. Limpert, "Gas-plasma-based generation of broadband terahertz radiation with 640 mW average power," *Opt. Lett.*, vol. 46, no. 20, p. 5256, Oct. 2021.

[15] J. Le, Y. Su, C. Tian, A. H. Kung, and Y. R. Shen, "A novel scheme for ultrashort terahertz pulse generation over a gapless wide spectral range: Raman-resonance-enhanced four-wave mixing," *Light: Sci. Appl.*, vol. 12, no. 1, p. 34, Feb. 2023.

[16] M. Kumar, H. S. Song, J. Lee, D. Park, H. Suk, and M. S. Hur, "Intense multicycle THz pulse generation from laser-produced nanoplasmas," *Sci. Rep.*, vol. 13, no. 1, p. 4233, Mar. 2023.

[17] N. Dessmann et al., "Highly efficient THz four-wave mixing in doped silicon," *Light: Sci. Appl.*, vol. 10, no. 1, p. 71, Apr. 2021.

[18] H. Wu, H. Liu, N. Huang, Q. Sun, and J. Wen, "High-power picosecond terahertz-wave generation in photonic crystal fiber via four-wave mixing," *Appl. Opt.*, vol. 50, no. 27, p. 5338, Sep. 2011.

[19] Z. Wang, H. Liu, N. Huang, Q. Sun, and J. Wen, "Efficient terahertz-wave generation via four-wave mixing in silicon membrane waveguides," *Opt. Exp.*, vol. 20, no. 8, p. 8920, Apr. 2012.

[20] H. Pakarzadeh and F. Akbari, "Propagation of terahertz pulses in photonic crystal-based rib silicon waveguides," *Silicon*, vol. 14, no. 6, pp. 2931–2940, Mar. 2021.

[21] H. Pakarzadeh and M. Bahrami, "Infrared to terahertz supercontinuum generation in a silicon-based rib waveguide," *J. Nonlinear Opt. Phys. Mater.*, 2025.

[22] L. Peters et al., "Resonant fully dielectric metasurfaces for ultrafast terahertz pulse generation," in *Proc. EPJ Web Conf.*, vol. 309, Apr. 2024, p. 08008.

[23] A. Kodigala, T. Lepetit, Q. Gu, B. Bahari, Y. Fainman, and B. Kanté, "Lasing action from photonic bound states in continuum," *Nature*, vol. 541, no. 7636, pp. 196–199, Jan. 2017.

[24] J. Bravo-Abad, A. W. Rodriguez, J. D. Joannopoulos, P. T. Rakich, S. G. Johnson, and M. Soljačić, "Efficient low-power terahertz generation via on-chip triply-resonant nonlinear frequency mixing," *Appl. Phys. Lett.*, vol. 96, no. 10, Mar. 2010, Art. no. 101110.

[25] T. Chen, J. Sun, L. Li, J. Tang, and Y. Zhou, "Design of a photonic crystal waveguide for terahertz-wave difference-frequency generation," *IEEE Photon. Technol. Lett.*, vol. 24, no. 11, pp. 921–923, Jun. 2012.

[26] Z. Lin, T. Alcorn, M. Loncar, S. G. Johnson, and A. W. Rodriguez, "High-efficiency degenerate four-wave mixing in triply resonant nanobeam cavities," *Phys. Rev. A, Gen. Phys.*, vol. 89, no. 5, May 2014, Art. no. 053839.

[27] P. Franceschini et al., "Enhancing second harmonic generation by Q-boosting lossless cavities beyond the time bandwidth limit," *Nanophotonics*, vol. 13, no. 1, pp. 1–8, Jan. 2024.

[28] P. Franceschini et al., "Intrapulse multimodal four-wave sum mixing in the visible range from high contrast index grating with PMMA layer," *Light: Sci. Appl.*, vol. 15, no. 1, p. 51, Jan. 2026.

[29] W. K. Burns and N. Bloembergen, "Third-harmonic generation in absorbing media of cubic or isotropic symmetry," *Phys. Rev. B, Condens. Matter*, vol. 4, no. 10, pp. 3437–3450, Nov. 1971.

[30] F. Preda, V. Kumar, F. Crisafi, D. G. Figueroa del Valle, G. Cerullo, and D. Polli, "Broadband pump-probe spectroscopy at 20-MHz modulation frequency," *Opt. Lett.*, vol. 41, no. 13, p. 2970, Jun. 2016.

Open Access funding provided by 'Università degli Studi di Palermo' within the CRUI CARE Agreement